International Journal of Chemical, Materials and Biomolecular Sciences
ISSN: 2415-6620
Vol:10, No:10, 2016

Preparation and Characterization of $CuFe_2O_4/TiO_2$ Photocatalyst for the Conversion of CO_2 into Methanol under Visible Light

Md. Maksudur Rahman Khan, M. Rahim Uddin, Hamidah Abdullah, Kaykobad Md. Rezaul Karim, Abu Yousuf, Chin Kui Cheng, Huei Ruey Ong

***Abstract*—**A systematic study was conducted to explore the photocatalytic reduction of carbon dioxide (CO_2) into methanol on TiO_2 loaded copper ferrite ($CuFe_2O_4$) photocatalyst under visible light irradiation. The phases and crystallite size of the photocatalysts were characterized by X-ray diffraction (XRD) and it indicates $CuFe_2O_4$ as tetragonal phase incorporation with anatase TiO_2 in $CuFe_2O_4/TiO_2$ hetero-structure. The XRD results confirmed the formation of spinel type tetragonal $CuFe_2O_4$ phases along with predominantly anatase phase of TiO_2 in the $CuFe_2O_4/TiO_2$ hetero-structure. UV-Vis absorption spectrum suggested the formation of the hetero-junction with relatively lower band gap than that of TiO_2. Photoluminescence (PL) technique was used to study the electron–hole (e^-/h^+) recombination process. PL spectra analysis confirmed the slow-down of the recombination of electron–hole (e^-/h^+) pairs in the $CuFe_2O_4/TiO_2$ hetero-structure. The photocatalytic performance of $CuFe_2O_4/TiO_2$ was evaluated based on the methanol yield with varying amount of TiO_2 over $CuFe_2O_4$ (0.5:1, 1:1, and 2:1) and changing light intensity. The mechanism of the photocatalysis was proposed based on the fact that the predominant species of CO_2 in aqueous phase were dissolved CO_2 and HCO_3^- at pH ~5.9. It was evident that the $CuFe_2O_4$ could harvest the electrons under visible light irradiation, which could further be injected to the conduction band of TiO_2 to increase the life time of the electron and facilitating the reactions of CO_2 to methanol. The developed catalyst showed good recycle ability up to four cycles where the loss of activity was ~25%. Methanol was observed as the main product over $CuFe_2O_4$, but loading with TiO_2 remarkably increased the methanol yield. Methanol yield over $CuFe_2O_4/TiO_2$ was found to be about three times higher (651 μmol/g_{cat} L) than that of $CuFe_2O_4$ photocatalyst. This occurs because the energy of the band excited electrons lies above the redox potentials of the reaction products CO_2/CH_3OH.

***Keywords*—**Photocatalysis, $CuFe_2O_4/TiO_2$, band-gap energy, methanol.

Md. Maksudur Rahman Khan is with the Faculty of Chemical and Natural Resources Engineering, Universiti Malaysia Pahang, 26300 Gambang, Pahang (phone: +609-549 2872; fax: +609-549 2889; e-mail: mrkhancep@yahoo.com).

M. Rahim Uddin, Hamidah Abdullah, Kaykobad Md. Rezaul Karim, Chin Kui Cheng, and Huei Ruey Ong are with the Faculty of Chemical and Natural Resources Engineering, Universiti Malaysia Pahang, 26300 Gambang, Pahang (e-mail: rahimuddin.cep@gmail.com, hamidahyusoff81@gmail.com, kaykobad1@gmail.com, chinkui@ump.edu.my, roi_rui86@hotmail.com).

Abu Yousuf is with the Faculty of Engineering Technology, Universiti Malaysia Pahang, 26300 Gambang, Pahang (e-mail: ayousufcep@yahoo.com).

I. Introduction

COMBUSTION of fossil fuel can be considered as the main power source for the growth of human civilization and no wonder, fossil fuel is the largest single source of energy consumed by the world's population. The reliance on fossil fuel for rapid industrialization cause unavoidable CO_2 emission [1]-[3]. CO_2 is the most concentrated greenhouse gas emitted by many industries, e.g. urea fertilizer industry, produce 100% CO_2 in flue gas [4], [5]. Therefore, carbon capture, storage and conversion into hydrocarbon technologies are drawing the attention of many researchers [3], [6].

Numerous methods have been explored to convert CO_2, such as hydrothermal, electrochemical and photochemical reduction of CO_2 to hydrocarbons. Hydrothermal reduction process requires high temperature (~450ºC) and pressure (25 MPa), hence it is energy intensive and costly [5], [7], [8]. The reduction of CO_2 by photocatalysts is one of the most promising methods for CO_2 reduction into methanol, especially under visible light irradiation [9-12].

Titanium dioxide (TiO_2), the most commonly used photocatalyst, is active under UV-light due to its large bandgap (~3.2 eV). Various methods have been studied to reduce the bandgap if TiO_2, such as doping with metals, non-metals and composite semiconductors on to TiO_2 [2], [7], [13]. The pre-requisites for the visible light active catalyst for the selective conversion of CO_2 to methanol under visible light are as follows: increased visible light absorption by decreasing the band gap [1], efficient charge separation and most importantly, the shift of the conduction band (CB) to more negative regions than the standard potentials for CO_2 reduction reactions [1], [8], [14]. The following reactions occur in the aqueous phase during CO_2 reduction to methanol [3], [9], [11]:

$$H_2O \rightarrow 0.5O_2 + 2H^+ + 2e^- \qquad E^0ox=1.23V \quad (1)$$

$$H^+ + e^- \rightarrow \tfrac{1}{2} H_2 \qquad E^0ox=0.0V \quad (2)$$

$$CO_2 + 6H^+ + 6e^- \rightarrow CH_3OH + H_2O \qquad E^0ox=-0.39V \quad (3)$$

So far, a variety of semiconductors including TiO_2 loaded composite and others catalysts like CdS/TiO_2, $FeTiO_3/TiO_2$, $CuO–TiO_2$, $Pt–TiO_2/MgO$, TiO_2/ZnO, $AgBr/TiO_2$, Cu/TiO_2, RuO_2/TiO_2 etc. have been reported as photocatalysts and these

types of hetero-junction helps to enhance the CO_2 reduction in aqueous phase reaction [7], [9], [15]-[17].

In our recent work, we demonstrated that the nanostructured $CuFe_2O_4$ and its further combination with TiO_2 can efficiently reduce CO_2 to methanol under visible light [18]. However, the effect of TiO_2 loading in the $CuFe_2O_4/TiO_2$, light intensity and catalyst loading on methanol yield has never been reported. In this study, $CuFe_2O_4/TiO_2$ photocatalysts were synthesized with different $CuFe_2O_4/TiO_2$ ratio and their photocatalytic activity for CO_2 reduction under visible light was evaluated. The recyclability of the catalysts has also been investigated.

II. Experimental Procedure

A. Materials

Copper nitrate, $Cu(NO_3)_2.3H_2O$ (99%), iron nitrate, $Fe(NO_3)_3.9H_2O$ (99%), Nitric acid, HNO_3 (65%), KOH, Agar, commercial TiO_2, KOH, and $NaNO_2$ were of analytical grade (R&M Marketing, Essex, UK) and used without further purification.

B. Catalyst Synthesis

$CuFe_2O_4$ photocatalyst was prepared using sol-gel method with slight modification of reaction conditions reported by [1]. For the preparation of $CuFe_2O_4$ catalyst, required amount of $Cu(NO_3)_2.3H_2O$ and $Fe(NO_3)_3.9H_2O$ were dissolved in 400 mL of water which contained HNO_3 (2M) and 4 g agar, and the solution was retained for 3 h under continuous stirring at room temperature. Thereafter, the temperature was raised to 90 ºC and stirred for ~3 h, where a green gel was obtained. The gel was dried at 130 ºC under vacuum for 24 h and grinded in a morter. The powder was calcined at 900 ºC with a heating rate of 10 ºC/min for 14 h as recommended by [1], [8], [19]. To prepare $CuFe_2O_4/TiO_2$ photocatalyst, $CuFe_2O_4$ was dispersed in 50 mL distilled water using ultrasound bath (Brand: Elmasonic S; Model: S10/S10H) and thereafter required amount of commercial TiO_2 was added. The ultrasonication was continued for another 1 h. In further, the suspension was dried overnight at 100 ºC in an oven. Afterward, the mixture was grinded and calcined at 700 ºC for 3 h in tubular furnace under N_2 gas atmosphere.

C. Instrumentations

The XRD patterns of the powders were obtained at room temperature using Rigaku MiniFlex II at Bragg angle of 2θ = 3-80° with a scan step of 0.02°. The measurements were performed at 30 kV and 15 mA using Cu–Kα emission and a nickel filter. The crystallite size of the prepared nanocomposite was also determined from the XRD spectra and the size was calculated by using the Scherrer formula [20]:

$$D = \frac{K\lambda}{B\cos\theta} \tag{4}$$

where, D is the coherent scattering length (crystallite size), K is a constant related to crystallite shape whose value is approximately 0.9 [20], λ is the X-ray wavelength of Cu–Kα radiation source = 0.15418 nm and B (in rad) is the full width at half-maximum (FWHM) of the peak, determined by Gaussian fitting. The morphologies of the prepared photocatalysts were observed by field emission scanning electron microscope (FE-SEM: model JEOL JSM-5410LV, Japan). Energy dispersive X-ray spectrometer (EDX) (5.0 kV) in connection with SEM was used to identify and analyze the elemental composition of photocatalysts. EDX patterns were also obtained using a JEOL JSM-7600, USA. UV–Vis absorption spectra of the samples were obtained by employing Shimadzu UV 2600 UV-Vis-NIR spectrophotometer. The N_2 adsorption–desorption experiments were conducted at 77 K in (Micromeritics ASAP 2020) Specific surface area (S_{BET}) of monolayer coverage was determined using Brunauer–Emmett–Teller (BET) method. Finally, the recombination rate of the photogenerated electron–hole pairs (e^-/h^+) was estimated using Perkin Elmer LS 55 Luminescence spectrophotometer. The catalysts are separated by centrifuging at 10000 rpm for 5 min using eppendorf centrifuge 5810 R.

Methanol in aqueous phase was analyzed by using Agilent gas chromatography (GC) with a flame ionization detector (FID) and the investigation was performed with Shimadzu, column DB-WAX 123-7033 (30 m×0.32 mm, 0.50 μm) and injected with a 7694 E headspace auto sampler.

D. Photocatalytic Activity

The photocatalytic reduction of CO_2 was performed in a continuous-flow reactor system as presented in Fig. 1. A reaction chamber was irradiated with a 500 W xenon lamp (light intensity 240 W/m^2) located in the middle of a quartz cool trap. Sodium nitrite solution (2M) was circulated through the quartz trap to cut the UV light in the range of 320 nm and 400 nm [9], [21], [22]. Firstly, 300 mL of distilled water was poured into the reactor and 1.2 g of KOH was dissolved in it to raise the pH to 12. Required amount of catalyst was added into the reactor to maintain the catalyst loading in the range of 0.5-2 g/L. Ultrapure CO_2 gas was bubbled through the solution for at least 1 h to ensure that all dissolved oxygen was eliminated and the pH of the solution was recorded as ~5.9. Thereafter, the lamp was switched on to start the photoreaction. The CO_2 was continuously bubbled throughout the process (8 h). The liquid sample was withdrawn using the vacuum pump and centrifuged at 10000 rpm for 5 min using Eppendorf centrifuge 5810 R. The supernatant was analyzed by GC-FID method.

III. Results and Discussion

A. XRD Analysis

The XRD patterns of as-prepared $CuFe_2O_4$ and $CuFe_2O_4/TiO_2$ photocatalysts are shown in Figs. 2 and 3, respectively. Fig. 2 illustrates that the diffraction patterns of the $CuFe_2O_4$ can be readily indexed as $CuFe_2O_4$ that has a good matching with JCPDS database (peak position of 101,112, 200, 202, 211, 220, 321, 224, 400, and 422). The spectra of the sample also indicate the presence of trace

amount of CuO (JCPDS 110, 200) phases. Fig. 3 illustrates the diffraction peaks of the $CuFe_2O_4/TiO_2$ photocatalysts that were calcined at 700°C and it also represents tetragonal, anatase TiO_2 (JCPDS 111, 102, 021, 022, 230, 620, 502, 532), and tetragonal $CuFe_2O_4$ (JCPDS 112, 202, 402, 221, 200, 312, 321, 224, 116 and 422).

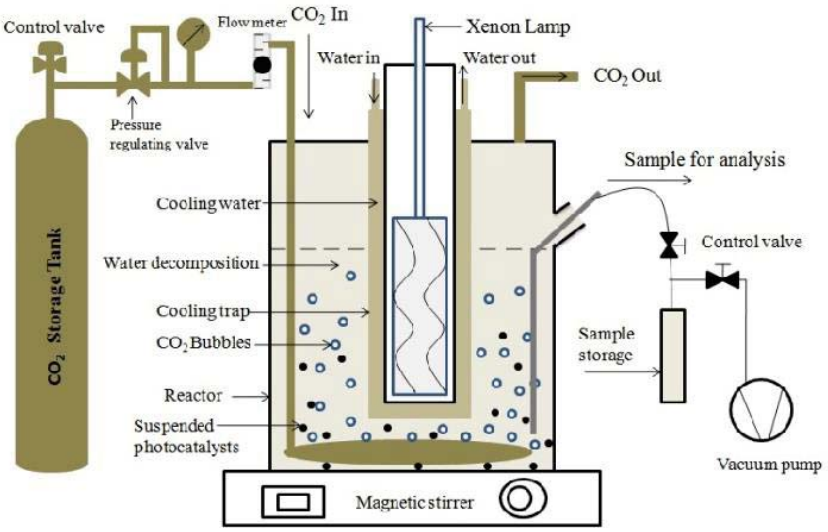

Fig. 1 Experimental setup for the photocatalytic conversion of CO_2 into methanol

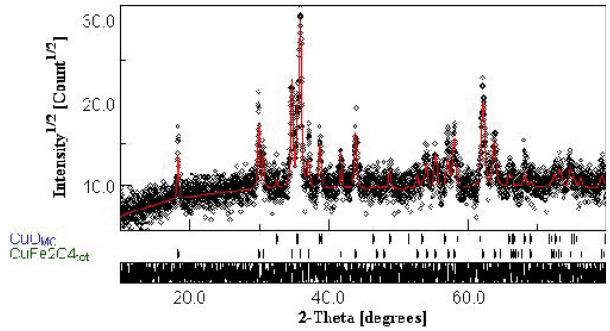

Fig. 2 XRD of as-prepared $CuFe_2O_4$

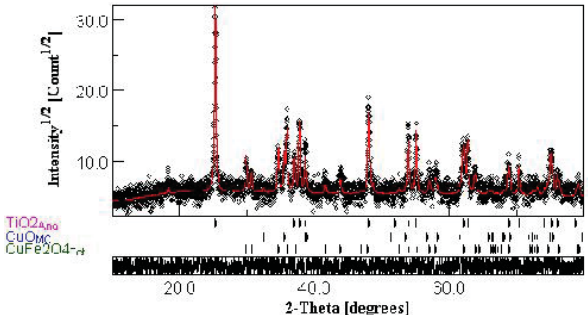

Fig. 3 XRD of as-prepared $CuFe_2O_4$–TiO_2

TABLE I
CRYSTALLOGRAPHIC PARAMETERS OF AS-PREPARED $CUFE_2O_4$ AND $CUFE_2O_4/TIO_2$ EXTRACTED FROM RIETVELD ANALYSIS

Sample	Phases	Composition (wt%)	symmetry	Space group	Lattice constant (Å)			Crystallite size (nm)	Microstrain	R%
					a	b	c			
$CuFe_2O_4$	$CuFe_2O_4$	85.33	Tetragonal	I41/amd:1	5.839	--	8.656	59	15.37E-4	16.65
	CuO	14.67	Monoclinic	C2/c:b1	4.688	3.425	5.135	67	4.02E-4	
$CuFe_2O_4/TiO_2$	$CuFe_2O_4$	18.06	Tetragonal	I41/amd:1	5.834	--	8.677	64	12.21E-4	19.55
	CuO	9.34	Monoclinic	C2/c:b1	4.688	3.426	5.134	98	3.38E-4	
	Anatase TiO_2	72.60	Tetragonal	I41/AMDS	3.786	--	9.514	108	2.21E-4	

According to the Scherrer formula in (4) the crystallite size of $CuFe_2O_4$ and $CuFe_2O_4/TiO_2$ photocatalysts were to be ~59 nm and ~108 nm (TiO_2) evaluated at $2\theta = 36.161^o$ (maximum intense peak). The crystallite size of TiO2 in prepared $CuFe_2O_4/TiO_2$ is higher (~19%) than that of $CuFe_2O_4$. A detailed description of phase constitution, lattice constants and micro structural parameters for as prepared samples is reported in Table I, as obtained from Rietveld refinement with a R% of about 16–20%. Together with the presence of tetragonal $CuFe_2O_4$ (85.33 wt%), the formation of a small amount of monoclinic CuO (14.67 wt%) is observed. In both cases, the lattice constants of $CuFe_2O_4$ are very similar to those reported in the crystallographic database (ICDD 340425) and that of CuO (ICDD 10706830) is reported as $a_0 = 4.684$, $b_0 = 3.425$ and $c_0 = 5.129$ Å. Anatase phase of TiO_2 of space group I41/AMDS observed at room temperature diffraction pattern and crystallographic parameters are very close to available database (ICDD 211272, $a_0 = 3.789$ and $c_0 = 9.537$ Å). Rietveld refinement shows that the as-prepared nanocomposite is free from more stable rutile TiO_2. It is, in

general, accepted that anatase shows more activity than rutile, in most photocatalytic reaction systems [23], may be due to the fact that the Fermi level of anatase is higher than that of rutile and slow recombination of e^- and h^+ [24].

B. UV-Vis Spectroscopy

The UV–Vis spectroscopy of the as-prepared $CuFe_2O_4$ and $CuFe_2O_4/TiO_2$ and commercial TiO_2 in the wavelength range of 250-1400 nm has been presented in Fig. 4 (a). Fig. 4 (a) shows transparency for wavelengths above 400, 480, 1010 nm which represents the visible light activity of the prepared photocatalysts. Plotting $(\alpha h\upsilon)^2$ versus $h\upsilon$ (Catalysts are presented as a direct transition) [25] based on the spectral response from Fig. 4 (a) gives the extrapolated intercept corresponding to the band gap energy value as shown in Fig. 4 (b), and Plotting $(\alpha h\upsilon)^{1/2}$ versus $h\upsilon$ (indirect transition) as shown in Fig. 4 (c). Figs. 4 (b) and (c) depict the band-gap of commercial TiO_2 (3.1 eV), $CuFe_2O_4/TiO_2$ (2.61 eV), and $CuFe_2O_4$ (1.24 eV). The optical band gap energy of $CuFe_2O_4/TiO_2$ is 2.61 eV which also display lower value compared to TiO_2 (3.1 eV). Kezzim et al. [1] reported the band gap of $CuFe_2O_4$ synthesized via sol–gel approach as 1.42 eV. Ahmed et al. [26] studied the suitable UV–visible light region (300-430 nm) for photocatalytic reduction of CO_2 into methanol. When a metal or composite is doped or loaded to the other composite, the previous band-gap was shifted to a new band-gap [2], [7]. In our prepared $CuFe_2O_4/TiO_2$ catalyst, the absorption edge of TiO_2 shifted from 400 to 480 nm due to the loading effect. A small shoulder exists at 350 to 367 nm as shown in Fig. 4 (a) for the $CuFe_2O_4/TiO_2$ photocatalyst; it may be due to the interaction of TiO_2 with $CuFe_2O_4$. The band gap of the recycled (after 4-time use, e.g. 4th recycle) catalyst was found to be shifted towards higher band gap (2.71 eV), might be due to the leaching of CuO or $CuFe_2O_4$ from the hetero-junction, which could not be confirmed in the present paper.

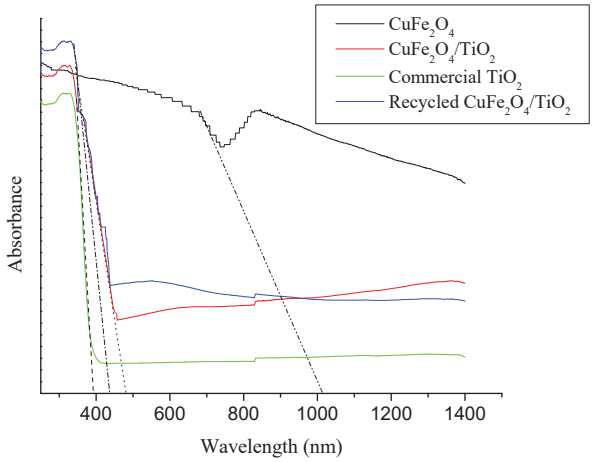

Fig. 4 (a) UV–Vis spectrum of prepared photocatalysts, the wavelength range was 250–1400 nm

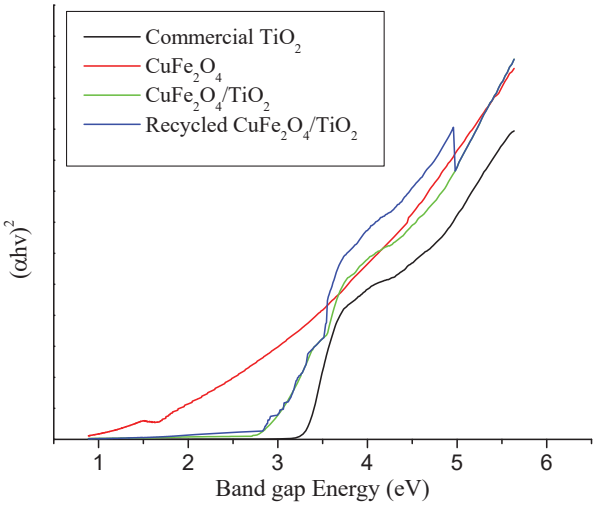

Fig. 4 (b) Band gap energy calculation of prepared photocatalysts (direct transition)

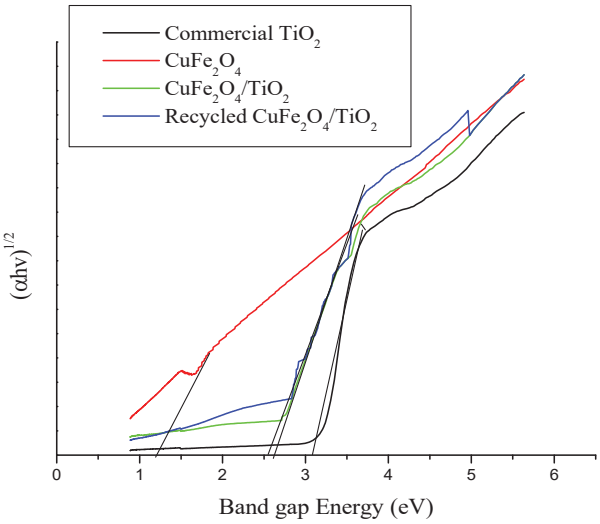

Fig. 4 (c) Band gap energy calculation of prepared photocatalysts (indirect transition)

C. PL Spectroscopy

The electron–hole (e^-/h^+) recombination process studied by PL spectroscopy. Fig. 5 compares PL spectra for $CuFe_2O_4$ and $CuFe_2O_4/TiO_2$, commercial TiO_2 and recycled $CuFe_2O_4/TiO_2$ catalyst (after four cycle of recycling process). $CuFe_2O_4/TiO_2$ photocatalyst exhibited a wide and strong PL signals in the range of 400-480 nm with the excited wavelength of 350 nm. The spectral peak located at 421 and 475 nm corresponds to anatase TiO_2 and effect of TiO_2 loading on $CuFe_2O_4$ while two peaks at 450 and 466 nm are attributed to the transition from the oxygen vacancies with two and one trapped electron to the $CuFe_2O_4$ conduction band (CB), respectively. However, TiO_2 band is more intense while the $CuFe_2O_4/TiO_2$ band intensities gradually weakened suggesting the lowering of e-/h+ recombination due to the $CuFe_2O_4$ loading with TiO_2. Furthermore, the recycled (after 4-time use, e.g. 4th recycle)

catalyst showed low PL intensity, but needed longer wavelength (very close to the TiO_2 spectrum), suggesting the loss of visible light active $CuFe_2O_4$ or CuO from the system. The result is consistent with the UV-Vis finding.

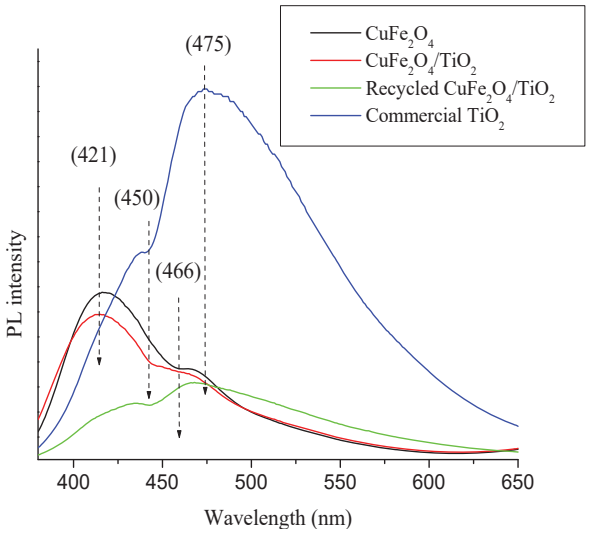

Fig. 5 PL emission spectra of $CuFe_2O_4$, $CuFe_2O_4/TiO_2$, commercial TiO_2 and recycled $CuFe_2O_4/TiO_2$catalyst (after four cycle of recycling process) photocatalysts; Excitation at 350 nm

D.Adsorption Isotherms, Surface Area (BET) and EDX Analysis

BET and EDX analysis of $CuFe_2O_4$ and $CuFe_2O_4/TiO_2$ is presented in Table II. The BET method is widely used for measuring the specific surface area of catalyst as presented in Fig. 6. Fig. 6 exhibits the N_2 adsorption–desorption isotherms of $CuFe_2O_4$ and $CuFe_2O_4/TiO_2$ photocatalysts. The mesoporous structure of $CuFe_2O_4$ and $CuFe_2O_4/TiO_2$ samples without surface directing agents were evidently due to the controlled hydrolysis process. Furthermore, the initial part of the isotherms (at low P/P_o) is related to the monolayer–multilayer adsorption on the internal surface. However, at higher P/P_o, the steep increment in the adsorption volume is attributed to the capillary condensation as the pores were saturated with liquid. This finding indicated that capillary condensation of nitrogen was occurred within the pores of the catalyst. The obtained BET surface area, average pore diameter and specific pore volume of $CuFe_2O_4$ were 1.49 m^2g^{-1}, 33.62 Å and, 0.0012 cm^3g^{-1}, and the BET surface area, average pore diameter and specific pore volume of $CuFe_2O_4/TiO_2$ were 1.98 m^2g^{-1}, 255.24 Å, and 0.013 cm^3g^{-1}, respectively. The low surface area for metal ferrites was also reported in literatures. The BET surface area of $NiFe_2O_4$ was 2.13 m^2g^{-1} and Co and Mn ferrite BET surface area was 2 m^2g^{-1} [27]-[29].

TABLE II
SURFACE AREA AND EDX ANALYSIS OF BARE $CUFE_2O_4$ AND TIO_2 LOADED $CUFE_2O_4/TIO_2$ SAMPLES

Sample	Surface area(m^2g^{-1})	Average pore diameter (Å)	Specific pore volume (cm^3g^{-1})	Surface elemental contents[a] (wt.%)			
				Cu	Fe	O	Ti
$CuFe_2O_4$	1.48	33.62	0.0012	21	57	22	-
$CuFe_2O_4/TiO_2$ (1:1 wt. ratio)	1.98	255.24	0.013	15.1	48.2	30.5	6.2

[a] Surface elemental contents calculated using EDX

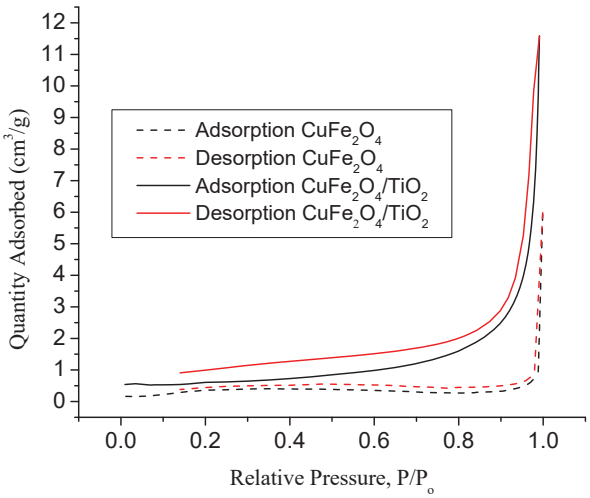

Fig. 6 N_2 adsorption-desorption isotherm of $CuFe_2O_4$ and $CuFe_2O_4/TiO_2$ photocatalyst

E. FE-SEM Analysis

Figs. 7 (a) and (b) portray the FE-SEM micrographs of $CuFe_2O_4$ and $CuFe_2O_4/TiO_2$ photocatalysts. The uniform shape of the mesoporous spherical particles can be attributed to the $CuFe_2O_4$ crystal growth due to controlled gel formation process. EDX analysis confirmed the appearance of peaks of Cu, Fe, O, Ti in the $CuFe_2O_4$ and TiO_2 loaded $CuFe_2O_4$ sample.

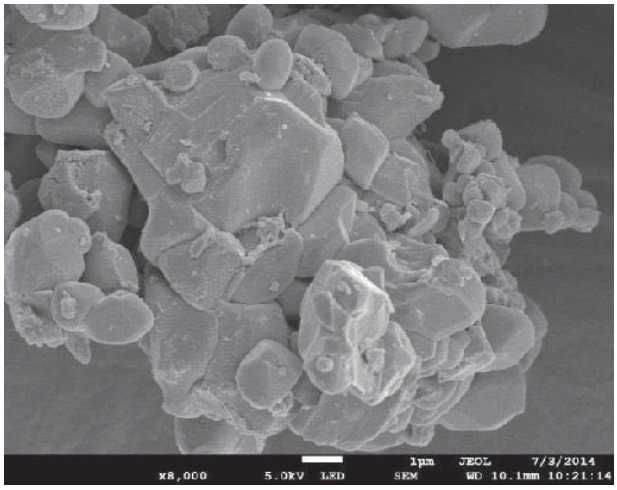

(a)

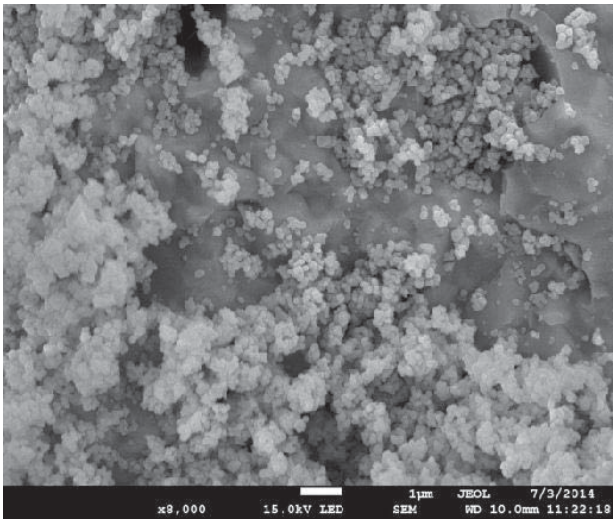

(b)

Fig. 7 FE-SEM micrograph of (a) $CuFe_2O_4$and (b) $CuFe_2O_4/TiO_2$prepared by sol–gel method

F. Photocatalytic Reduction of CO_2: Effect of TiO_2 Loading on $CuFe_2O_4$

The photocatalytic reduction of CO_2 and successive formation of methanol was investigated over a period of 8 h irradiation on $CuFe_2O_4/TiO_2$ and $CuFe_2O_4$ photocatalysts as shown in Fig. 8. The experimental result showed the methanol as the main product in the liquid phase. Hydrogen, CO, formaldehyde, ethane and ethylene could also be formed according to the reports in the literature [6], [9], [26], but they were undetectable in our case. Fig. 8 depicts that the highest methanol yield (651 μmol/g_{cat} L) was obtained for $CuFe_2O_4/TiO_2$ (1:1 weight ratio) photocatalyst, compare to that of (220 μmol/g_{cat}) $CuFe_2O_4$ after 8 h of reaction. A slight decline of the catalyst activity after 6h of reaction, both catalysts indicated the unavailability of the active sites or the deactivation of the catalyst. The yield of methanol with $CuFe_2O_4/TiO_2$ for the photocatalytic reduction of CO_2 under visible light was significantly higher than the results presented in literature [6].

G.Photocatalytic Reduction of CO_2: Effect of Catalyst Loading for CO_2 Reduction

To study the effect of catalyst loading on methanol yield, the catalyst loading was varied from 0.5 to 2 g/L. The results are presented in Fig. 9. From the figure, the methanol yield was increased with the increase in catalyst loading. The highest yield of methanol for $CuFe_2O_4/TiO_2$ photocatalyst was 695 μmol/g_{cat}L at 2 g/L catalyst loading after 6 h irradiation. In comparison with the 1 g/L catalyst loading the methanol yield was increased only 6.8% by doubling the catalyst amount into the solution. According to the figure, in case of increasing the catalyst loading from 0.5 g/L to 1 g/L, methanol production was drastically raised to around 70% but further increasing of catalyst loading yield was not significant might be due to the exhaustion of the active sites. The result is consistent with the literature finding where 1 g/L showed the optimum methanol yield [7], [22], [30].

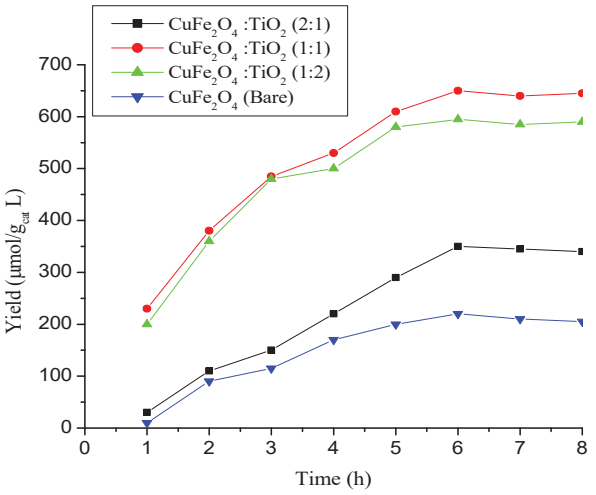

Fig. 8 Effect of $CuFe_2O_4/TiO_2$ ratio for photocatalytic reduction of CO_2 to methanol under visible light irradiation for 8 h

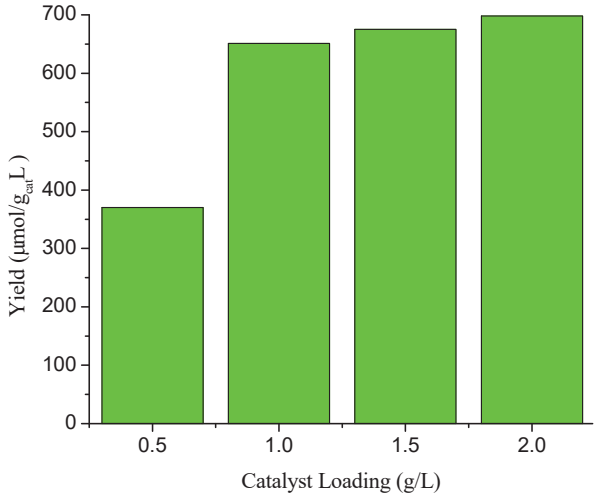

Fig. 9 Effect of catalyst loading for CO_2 conversion at 6 h irradiation (Light intensity = 240 W/m^2)

H.Photocatalytic Reduction of CO_2: Effect of Light Intensity for CO_2 Reduction

The effect of visible light intensity on photocatalytic CO_2 reduction process is presented in Fig. 10. Fig. 10 illustrates the direct effect of the light intensity on photocatalytic reduction of CO_2 into methanol for 8 h irradiation period. After increasing the light intensity methanol yield was significantly increased about 14% (at 8 h irradiation). The light intensity of 249 W.m^{-2} was chosen as optimum, as further increase in light intensity could not increase the methanol yield.

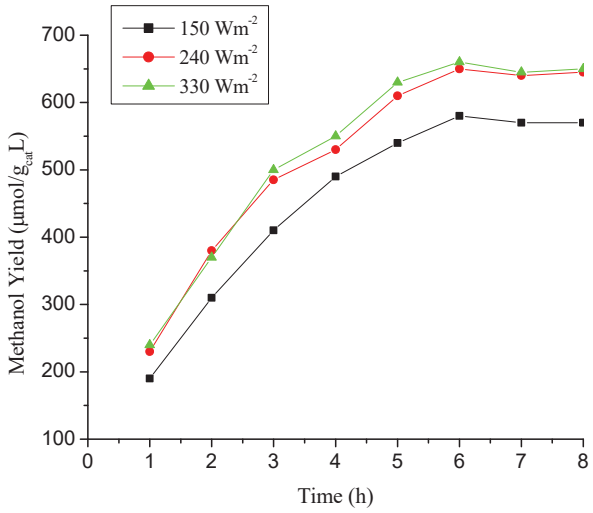

Fig. 10 Effect of light intensity on CO_2 conversion to methanol under visible light irradiation for 8 h (catalyst loading = 1gL^{-1})

I. Recycling of Catalyst for CO_2 Reduction

The catalyst recycling for four different cycles was performed and presented at Fig. 11. After each run, the whole reaction mixture was centrifuged, before reuse in the second reaction cycle; the recovered catalyst was dried over night at 100 °C and subsequently used for new cycle under the optimum operating conditions. It was observed that the catalyst activity gradually decreased during 8 h irradiation (Fig. 11) and the activity was decreased about 25.6% after four cycles of operation compare to the first cycle. The UV-visible and PL data suggested the loss of active phase in the recycled catalysts might be the reason for the reduction of the activity.

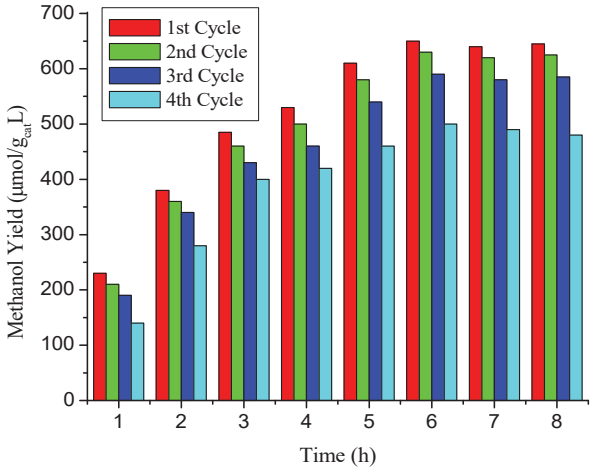

Fig. 11 Effect of catalyst recycles on methanol production over $CuFe_2O_4/TiO_2$ (each cycle duration = 8 h; Light intensity = 240 Wm^{-2}; room temperature

J. Mechanism of Methanol Formation

The mechanism of methanol formation over prepared $CuFe_2O_4$ and $CuFe_2O_4/TiO_2$ photocatalysts are shown in Fig. 11. At pH ~ 5.9, CO_2 may exist as dissolved CO_2 and HCO_3^-, but the predominant species at low pH are the dissolved CO_2 and HCO_3^- [31].

As shown in Fig. 12, the reduction potential of the possible reactions of these species of CO_2 falls in between the VB and CB of both $CuFe_2O_4$ and $CuFe_2O_4/TiO_2$ suggesting that the reaction can occur on both photocatalysts [9], [32]. Comparing the band gap, $CuFe_2O_4$ (1.24 eV) is more visible light active than the TiO_2 (3.1 eV). According to the standard reaction potential (E^0ox= -0.39 V), the of methanol formation alone on $CuFe_2O_4$ is low due to the large difference between the potential of the CB (- 1.03 V) of $CuFe_2O_4$ and the redox couple (-0.38 V). Under visible light, excited e^- could move from VB to CB of $CuFe_2O_4$ whereas CB (-1.03 V) edge of $CuFe_2O_4$ is higher than that of the TiO_2 CB (-0.97 V), the excited e^- can easily transferred to the CB of TiO_2 in $CuFe_2O_4/TiO_2$ hetero-structure where the CO_2 reduction can take place. The hetero-structure should increase the e^- life time by suppressing the e^-/h^+ recombination. The reduction of the e^-/h^+ recombination rate in the hetero-structure was evident from Fig. 5. Therefore, $CuFe_2O_4/TiO_2$ hetero-structure can promote the charge pair separation and prolong the recombination of e^-/h^+ pairs resulting in higher CO_2 reduction efficiency.

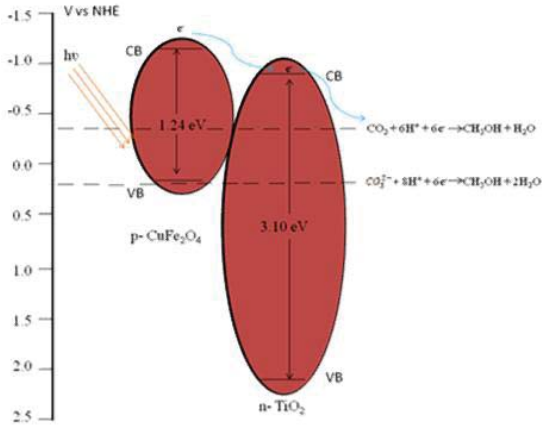

Fig. 12 The mechanism of CO_2 reduction to methanol over prepared $CuFe_2O_4$ and $CuFe_2O_4/TiO_2$ photocatalysts

IV. Conclusions

In summary, significant enhancement of the photocatalytic reduction of CO_2 under visible light irradiation was observed when TiO_2 was deposited on $CuFe_2O_4$. The catalyst composition and the reaction parameters were studied for methanol production and optimum $TiO_2/CuFe_2O_4$ ratio, catalysts loading and light intensity were found as 1/1, 1 gL^{-1} and 240 Wm^{-2} respectively. The XRD patterns of $CuFe_2O_4$ and $CuFe_2O_4/TiO_2$ confirmed their tetragonal structure, and crystallite sizes of ~59 nm ($CuFe_2O_4$) and ~108 nm (TiO_2), respectively. The modification of $CuFe_2O_4$ with TiO_2, enhanced its photocatalytic activity by shifting the band-gap of commercial TiO_2 (3.1 eV) into a new band-gap of $CuFe_2O_4/TiO_2$ (2.61 eV) photocatalyst, enabling the generation of photo electron under visible light. $CuFe_2O_4/TiO_2$ showed lower e^-/h^+ recombination compared to $CuFe_2O_4$. The

maximum yield of methanol over $CuFe_2O_4$ and $CuFe_2O_4/TiO_2$ photocatalysts under visible light irradiation were 220 and 651 $\mu mol/g_{cat}$ L, respectively.

ACKNOWLEDGMENT

The authors would like to thank the Malaysian Ministry of Education for Fundamental Research Grant Scheme (RDU150118) and Universiti Malaysia Pahang for funding (GRS140330).

REFERENCES

[1] A. Kezzim, N. Nasrallah, A. Abdi, M. Trari, "Visible light induced hydrogen on the novel hetero-system $CuFe_2O4/TiO_2$," Energy Conversion and Management, vol. 52, no. 8–9, 2011, pp. 2800-2806.

[2] Y. Izumi, "Recent advances in the photocatalytic conversion of carbon dioxide to fuels with water and/or hydrogen using solar energy and beyond," Coordination Chemistry Reviews, vol. 257, no. 1, 2013, pp. 171-186.

[3] S. C. Roy, O. K. Varghese, M. Paulose, C. A. Grimes, "Toward solar fuels: photocatalytic conversion of carbon dioxide to hydrocarbons," ACS Nano, vol. 4, no. 3, 2010, pp. 1259-1278.

[4] Q. Zhang, C. F. Lin, B. Y. Chen, T. Ouyang, C. T. Chang, "Deciphering Visible Light Photoreductive Conversion of CO_2 to Formic Acid and Methanol Using Waste Prepared Material," Environ Sci Technol, vol. 49, no. 4, 2015, pp. 2405-2417.

[5] J. Mao, T. Peng, X. Zhang, K. Li, L. Zan, "Selective methanol production from photocatalytic reduction of CO_2 on $BiVO_4$ under visible light irradiation," Catalysis Communications, vol. 28, no. 2012, pp. 38-41.

[6] K. Kočí, K. Matějů, L. Obalová, S. Krejčíková, Z. Lacný, D. Plachá, L. Čapek, A. Hospodková, O. Šolcová, "Effect of silver doping on the TiO_2 for photocatalytic reduction of CO_2," Applied Catalysis B: Environmental, vol. 96, no. 3-4, 2010, pp. 239-244.

[7] M. Tahir, N. S. Amin, "Advances in visible light responsive titanium oxide-based photocatalysts for CO_2 conversion to hydrocarbon fuels," Energy Conversion and Management, vol. 76, no. 2013, pp. 194-214.

[8] H. Yang, J. Yan, Z. Lu, X. Cheng, Y. Tang, "Photocatalytic activity evaluation of tetragonal $CuFe_2O_4$ nanoparticles for the H2 evolution under visible light irradiation," Journal of Alloys and Compounds, vol. 476, no. 1-2, 2009, pp. 715-719.

[9] X. Li, J. Chen, H. Li, J. Li, Y. Xu, Y. Liu, J. Zhou, "Photoreduction of CO2 to methanol over Bi_2S_3/CdS photocatalyst under visible light irradiation," Journal of Natural Gas Chemistry, vol. 20, no. 4, 2011, pp. 413-417.

[10] A. Di Paola, M. Bellardita, L. Palmisano, "Brookite, the Least Known TiO2 Photocatalyst," Catalysts, vol. 3, no. 1, 2013, pp. 36-73.

[11] A. Di Paola, E. García-López, G. Marcì, L. Palmisano, "A survey of photocatalytic materials for environmental remediation," J Hazard Mater, vol. 211, no. 2012, pp. 3-29.

[12] W. Hou, W. H. Hung, P. Pavaskar, A. Goeppert, M. Aykol, S. B. Cronin, "Photocatalytic Conversion of CO_2 to Hydrocarbon Fuels via Plasmon-Enhanced Absorption and Metallic Interband Transitions," ACS Catalysis, vol. 1, no. 8, 2011, pp. 929-936.

[13] W.-N. Wang, J. Soulis, Y. J. Yang, P. Biswas, "Comparison of CO_2 photoreduction systems: A review," Aerosol and Air Quality Research, vol. 14, no. 2, 2014, pp. 533-549.

[14] M. L. P. Dalida, K. M. S. Amer, C.-C. Su, M.-C. Lu, "Photocatalytic degradation of acetaminophen in modified TiO_2 under visible irradiation," Environmental Science and Pollution Research, vol. 21, no. 2, 2014, pp. 1208-1216.

[15] H. Fan, H. Li, B. Liu, Y. Lu, T. Xie, D. Wang, "Photoinduced charge transfer properties and photocatalytic activity in $Bi_2O_3/BaTiO_3$ composite photocatalyst," ACS Appl Mater Interfaces, vol. 4, no. 9, 2012, pp. 4853-4857.

[16] D. Monllor-Satoca, R. Gomez, W. Choi, "Concentration-dependent photoredox conversion of As(III)/As(V) on illuminated titanium dioxide electrodes," Environ Sci Technol, vol. 46, no. 10, 2012, pp. 5519-5527.

[17] P. Roy, A. P. Periasamy, C. T. Liang, H. T. Chang, "Synthesis of graphene-ZnO-Au nanocomposites for efficient photocatalytic reduction of nitrobenzene," Environ Sci Technol, vol. 47, no. 12, 2013, pp. 6688-6695.

[18] M. R. Uddin, M. R. Khan, M. W. Rahman, A. Yousuf, C. K. Cheng, "Photocatalytic reduction of CO_2 into methanol over $CuFe_2O_4/TiO_2$ under visible light irradiation," Reaction Kinetics, Mechanisms and Catalysis, vol. 116, no. 2, 2015, pp. 589-604.

[19] J. Yan, H. Yang, Y. Tang, Z. Lu, S. Zheng, M. Yao, Y. Han, "Synthesis and photocatalytic activity of $CuYyFe_2$−yO4–$CuCo_2O_4$ nanocomposites for H2 evolution under visible light irradiation," Renewable Energy, vol. 34, no. 11, 2009, pp. 2399-2403.

[20] O. Lemine, "Microstructural characterisation of nanoparticles using, XRD line profiles analysis, FE-SEM and FT-IR," Superlattices and Microstructures, vol. 45, no. 6, 2009, pp. 576-582.

[21] L. Huang, F. Peng, H. Wang, H. Yu, Z. Li, "Preparation and characterization of Cu 2 O/TiO 2 nano–nano heterostructure photocatalysts," Catalysis Communications, vol. 10, no. 14, 2009, pp. 1839-1843.

[22] X. Li, H. Liu, D. Luo, J. Li, Y. Huang, H. Li, Y. Fang, Y. Xu, L. Zhu, "Adsorption of CO_2 on heterostructure $CdS(Bi_2S_3)/TiO_2$ nanotube photocatalysts and their photocatalytic activities in the reduction of CO_2 to methanol under visible light irradiation," Chemical Engineering Journal, vol. 180, no. 2012, pp. 151-158.

[23] M. Hussain, N. Russo, G. Saracco, "Photocatalytic abatement of VOCs by novel optimized TiO_2 nanoparticles," Chemical Engineering Journal, vol. 166, no. 1, 2011, pp. 138-149.

[24] J. T. Carneiro, T. J. Savenije, J. A. Moulijn, G. Mul, "How phase composition influences optoelectronic and photocatalytic properties of TiO_2," The Journal of Physical Chemistry C, vol. 115, no. 5, 2011, pp. 2211-2217.

[25] M. Tahir, N. S. Amin, "Indium-doped TiO_2 nanoparticles for photocatalytic CO_2 reduction with H_2O vapors to CH_4," Applied Catalysis B: Environmental, vol. 162, no. 2015, pp. 98-109.

[26] N. Ahmed, M. Morikawa, Y. Izumi, "Photocatalytic conversion of carbon dioxide into methanol using optimized layered double hydroxide catalysts," Catalysis Today, vol. 185, no. 1, 2012, pp. 263-269.

[27] D.-H. Chen, X.-R. He, "Synthesis of nickel ferrite nanoparticles by sol-gel method," Materials Research Bulletin, vol. 36, no. 7, 2001, pp. 1369-1377.

[28] C. G. Reddy, S. Manorama, V. Rao, "Preparation and characterization of ferrites as gas sensor materials," Journal of materials science letters, vol. 19, no. 9, 2000, pp. 775-778.

[29] I. Sandu, L. Presmanes, P. Alphonse, P. Tailhades, "Nanostructured cobalt manganese ferrite thin films for gas sensor application," Thin Solid Films, vol. 495, no. 1, 2006, pp. 130-133.

[30] L. L. Ma, H. Z. Sun, Y. G. Zhang, Y. L. Lin, J. L. Li, E. K. Wang, Y. Yu, M. Tan, J. B. Wang, "Preparation, characterization and photocatalytic properties of CdS nanoparticles dotted on the surface of carbon nanotubes," Nanotechnology, vol. 19, no. 11, 2008, pp. 115709.

[31] S. K. Lower, Carbonate equilibria in natural waters, in: Simon Fraser University, 1999.

[32] L. Liu, "Understanding the Reaction Mechanism of Photocatalytic Reduction of CO_2 with H_2O on TiO_2-Based Photocatalysts: A Review," Aerosol and Air Quality Research, vol. no. 2014, pp.